PHYSICAL REVIEW D **78,** 064021 (2008)

Testing alternative theories of dark matter with the CMB

Baojiu Li,[1,*] John D. Barrow,[1,+] David F. Mota,[2,‡] and HongSheng Zhao[3,§]

[1]*DAMTP, Centre for Mathematical Sciences, University of Cambridge, Cambridge CB3 0WA, United Kingdom*
[2]*Institute of Theoretical Physics, University of Heidelberg, 69120 Heidelberg, Germany*
[3]*Scottish University Physics Alliance, University of St. Andrews, KY16 9SS, United Kingdom*

(Received 28 May 2008; published 26 September 2008)

We propose a method to study and constrain modified gravity theories for dark matter using CMB temperature anisotropies and polarization. We assume that the theories considered here have already passed the matter power-spectrum test of large-scale structure. With this requirement met, we show that a modified gravity theory can be specified by parametrizing the time evolution of its dark-matter density contrast, which is completely controlled by the dark-matter stress history. We calculate how the stress history with a given parametrization affects the CMB observables, and a qualitative discussion of the physical effects involved is supplemented with numerical examples. It is found that, in general, alternative gravity theories can be efficiently constrained by the CMB temperature and polarization spectra. There exist, however, special cases where modified gravity cannot be distinguished from the CDM model even by using *both* CMB *and* matter power spectrum observations, nor can they be efficiently restricted by other observables in perturbed cosmologies. Our results show how the stress properties of dark matter, which determine the evolutions of both density perturbations and the gravitational potential, can be effectively investigated using just the general conservation equations and without assuming any specific theoretical gravitational theory within a wide class.

DOI: 10.1103/PhysRevD.78.064021 PACS numbers: 04.50.Kd, 95.35.+d, 98.70.Vc

I. INTRODUCTION

Various cosmological observations indicate that almost 95% of the energy content of our universe is in some dark form that can only be detected through its gravitational effects. The standard explanation for this ''dark sector'' involves some kind of cold dark matter (CDM), such as heavy weakly interacting particles or primordial black holes, and dark energy, which could be a manifestation of a cosmological constant (Λ) or some exotic matter field. This standard hybrid picture (ΛCDM) has so far passed several different cosmological tests, and is dubbed the ''concordance model.'' Despite its successes, however, it is not without problems in accounting for structure on galactic scales—for example, the greatest challenge is to form bulge-free bright spiral galaxies and dwarf spiral galaxies. The galaxies in CDM have either a dominating stellar bulge or a dominating CDM cusp at the center. In essence, ΛCDM over predicts the dark-matter effects required by the empirical Tully-Fisher relation of spiral galaxies—and is in need of an experimental identification of the CDM particles with an understanding of why the dark energy possesses its particular energy density.

Since dark energy affects cosmological models mainly via gravitational effects, it is possible to imagine that the effects of an explicit material source for the dark energy can be mimicked by a change in the behavior of the gravitational field at late times. This is an unusual requirement, since we have expected deviations from general relativity to arise in the high spacetime curvature limit at early times rather than in the low spacetime curvature limit at late times. However, we should note that the addition of an explicit cosmological constant to general relativity, as in the concordance model of ΛCDM, is already a particular example of such a low spacetime curvature correction. There have been many investigations of gravitational alternatives to dark energy [1–10], and it appears that most of these attempts create different problems in either local gravitational systems or large-scale structure (LSS) formation, or even both [11–26] (see [27–32] on possible ways to overcome these problems). In response to these investigations, frameworks to test modified gravitational dark energy models have also been developed [33–38].

The situation is nonetheless different in the dark-matter arena, where the leading modified gravity model, Milgrom's modified Newtonian dynamics (MOND) [39], appeared more than two decades ago, but lacked a convincing general-relativistic formulation with a set of relativistic field equations applicable to cosmology. This hurdle has recently been overcome by Bekenstein's tensor-vector-scalar (TeVeS) model [40], which reduces to MOND in the relevant limit. Actually, what the TeVeS model provides is more than a relativistic framework to investigate cosmology—it has been found that in TeVeS the formation of LSS, which was thought of as a problem for modified gravity theories before, could also be made consistent with observations [41,42]. Meanwhile, TeVeS has also been shown to work well on smaller scales (e.g.,

*b.li@damtp.cam.ac.uk
+j.d.barrow@damtp.cam.ac.uk
‡d.mota@thphys.uni-heidelberg.de
§hz4@st-andrews.ac.uk

mimicking cold dark matter in strong gravitational lensing systems [43,44], producing elliptical galaxies, barred spiral galaxies, and even tidal dwarf galaxies [45,46], being consistent with solar system tests and so on) and inherit the advantages of MOND over the CDM model [47] (e.g., in explaining the Tully-Fisher law and galaxy rotation curves), this discovery attracts much interest on TeVeS and its generalizations. Also, since TeVeS manages to grow large-scale structure using the growing mode of its vector field, this stimulates the investigation of vector-field cosmology [48] in general [49–57] (in Ref. [57], for example, a very general vector-scalar field framework, the so-called dark fluid, is proposed which can reduce to many existing models in appropriate limits), and it is found that the LSS in these theories could also be consistent with observations [58].

Despite this encouraging success, one should bear in mind that LSS only provides one test of any structure formation model. In fact, the matter (or galaxy) power spectrum we observe today only reflects the large-scale matter-density perturbation *today* (δ_{m0}), rather than its evolutionary history. Thus, even though the matter power spectrum $P(k)$ is compatible with observations, the evolution path of δ_m may well be different from that followed in the ΛCDM paradigm. This situation is shown particularly clearly in Fig. 3 (lower panel) of [42], where the growth rate of baryon density perturbations is enhanced only at late times. The different evolution history of matter-density perturbations may have significant impacts on various other cosmological observables, such as the cosmic microwave background (CMB) power spectrum, and influence the growth of nonlinear structure. We would like to determine what these impacts are.

In this paper we take a first step in that direction. We will concentrate on the influences of general modified gravity dark-matter models on CMB observables. Our main assumption is that the modification to general relativity (GR) can be expressed as an *effective dark matter* (EDM) term and moved to the right-hand side of the field equations so that the left-hand side is the same as in GR. This EDM term, like the standard CDM (SCDM), governs both the background and perturbation evolutions. This assumption is justified by observing the fact that in TeVeS, as well as in the general vector-field (or $f(K)$) theories, the terms involving the vector field are essentially just the EDM term described here. Furthermore, we make some simplifying assumptions. First, any explicit dark energy is neglected. The main effects of dark energy (if not too exotic in origin) are to modify the background evolution at late times and cause the decay of the large-scale gravitational potential. Neglecting it does not affect the essential features of our model but will simplify the numerics greatly. Second, the background evolution is exactly the same as that in the SCDM model, which should also be a good approximation. Third, the matter power spectrum, or equivalently δ_{m0}, is the same as that of SCDM, because any deviation from the latter should be stringently constrained by LSS observations, and because both TeVeS and $f(K)$ models have claimed to reproduce the observed matter power spectrum. Hence, we are fixing δ_{m0} and investigating how different evolutions of $\delta_m(a)$ (where a is the cosmic scale factor) affect the CMB power spectrum. Our theoretical framework is designed to be more general than is required for this purpose alone, and could be used to investigate features of other cosmological models.

This paper is organized as follows: in Sec. II, we set out the theoretical framework for our investigation and introduce more details of the cosmological model. In Sec. III, we describe briefly how a general dark-matter component affects the CMB power spectrum and then, in Sec. IV, supplement this discussion with a numerical example. We consider three special cases, which span all the possibilities in the model, and explain them one by one. Finally, in Sec. V, we provide a summary of our results together with some further discussion of the assumptions on which they are based.

II. THE THEORETICAL FRAMEWORK

In this analysis we use the perturbed Einstein equations in the covariant and gauge invariant (CGI) formalism.

A. The perturbation equations in CGI formalism

The CGI perturbation equations in general theories of gravity are derived in this section using the method of 3 + 1 decomposition [59]. First, we briefly review the main ingredients of 3 + 1 decomposition and their application to standard general relativity [59] for ease of later reference.

The main idea of 3 + 1 decomposition is to make spacetime splits of physical quantities with respect to the 4 velocity u^a of an observer. The projection tensor h_{ab} is defined as $h_{ab} = g_{ab} - u_a u_b$ and can be used to obtain covariant tensors perpendicular to u. For example, the covariant spatial derivative $\hat{\nabla}$ of a tensor field $T^{b\cdots c}_{d\cdots e}$ is defined as

$$\hat{\nabla}^a T^{b\cdots c}_{d\cdots e} \equiv h^a_i h^b_j \cdots h^c_k h^r_d \cdots h^s_e \nabla^i T^{j\cdots k}_{r\cdots s}. \tag{1}$$

The energy-momentum tensor and covariant derivative of the 4 velocity are decomposed, respectively, as

$$T_{ab} = \pi_{ab} + 2q_{(a}u_{b)} + \rho u_a u_b - p h_{ab}, \tag{2}$$

$$\nabla_a u_b = \sigma_{ab} + \varpi_{ab} + \tfrac{1}{3}\theta h_{ab} + u_a A_b. \tag{3}$$

In the above, π_{ab} is the projected symmetric trace-free anisotropic stress, q_a the vector heat flux vector, p the isotropic pressure, σ_{ab} the projected symmetric trace-free shear tensor, $\varpi_{ab} = \hat{\nabla}_{[a}u_{b]}$, the vorticity, $\theta = \nabla^c u_c \equiv 3\dot{a}/a$ (a is the mean expansion scale factor) the expansion scalar, and $A_b = \dot{u}_b$ the acceleration; the overdot denotes

time derivative expressed as $\dot{\phi} = u^a \nabla_a \phi$, brackets mean antisymmetrization, and parentheses symmetrization. The 4-velocity normalization is chosen to be $u^a u_a = 1$. The quantities π_{ab}, q_a, ρ, p are referred to as *dynamical* quantities and σ_{ab}, ϖ_{ab}, θ, A_a as *kinematical* quantities. Note that the dynamical quantities can be obtained from the energy-momentum tensor T_{ab} through the relations

$$\begin{aligned} \rho &= T_{ab}u^a u^b, \qquad p = -\tfrac{1}{3}h^{ab}T_{ab}, \\ q_a &= h_a^d u^c T_{cd}, \qquad \pi_{ab} = h_a^c h_b^d T_{cd} + p h_{ab}. \end{aligned} \tag{4}$$

Decomposing the Riemann tensor and making use the Einstein equations, we obtain, after linearization, five constraint equations [59]:

$$0 = \hat{\nabla}^c(\varepsilon^{ab}{}_{cd} u^d \varpi_{ab}); \tag{5}$$

$$\kappa q_a = -\frac{2\hat{\nabla}_a \theta}{3} + \hat{\nabla}^b \sigma_{ab} + \hat{\nabla}^b \varpi_{ab}; \tag{6}$$

$$\mathcal{B}_{ab} = [\hat{\nabla}^c \sigma_{d(a} + \hat{\nabla}^c \varpi_{d(a}]\varepsilon_{b)ec}{}^d u^e; \tag{7}$$

$$\hat{\nabla}^b \mathcal{E}_{ab} = \frac{1}{2}\kappa\left[\hat{\nabla}^b \pi_{ab} + \frac{2}{3}\theta q_a + \frac{2}{3}\hat{\nabla}_a \rho\right]; \tag{8}$$

$$\hat{\nabla}^b \mathcal{B}_{ab} = \frac{1}{2}\kappa[\hat{\nabla}_c q_d + (\rho + p)\varpi_{cd}]\varepsilon_{ab}{}^{cd} u^b, \tag{9}$$

and five propagation equations

$$\dot{\theta} + \frac{1}{3}\theta^2 - \hat{\nabla}^a A_a + \frac{\kappa}{2}(\rho + 3p) = 0; \tag{10}$$

$$\dot{\sigma}_{ab} + \frac{2}{3}\theta\sigma_{ab} - \hat{\nabla}_{\langle a} A_{b\rangle} + \mathcal{E}_{ab} + \frac{1}{2}\kappa\pi_{ab} = 0; \tag{11}$$

$$\dot{\varpi} + \frac{2}{3}\theta\varpi - \hat{\nabla}_{[a} A_{b]} = 0; \tag{12}$$

$$\begin{aligned} &\frac{1}{2}\kappa\left[\dot{\pi}_{ab} + \frac{1}{3}\theta\pi_{ab}\right] - \frac{1}{2}\kappa[(\rho + p)\sigma_{ab} + \hat{\nabla}_{\langle a} q_{b\rangle}] \\ &\quad - [\dot{\mathcal{E}}_{ab} + \theta\mathcal{E}_{ab} - \hat{\nabla}^c \mathcal{B}_{d(a}\varepsilon_{b)ec}{}^d u^e] = 0; \end{aligned} \tag{13}$$

$$\dot{\mathcal{B}}_{ab} + \theta\mathcal{B}_{ab} + \hat{\nabla}^c \mathcal{E}_{d(a}\varepsilon_{b)ec}{}^d u^e + \frac{\kappa}{2}\hat{\nabla}^c \pi_{d(a}\varepsilon_{b)ec}{}^d u^e = 0. \tag{14}$$

Here, ε_{abcd} is the covariant permutation tensor, $\mathcal{E}_{ab}$ and $\mathcal{B}_{ab}$ are, respectively, the electric and magnetic parts of the Weyl tensor $\mathcal{W}_{abcd}$, defined by $\mathcal{E}_{ab} = u^c u^d \mathcal{W}_{acbd}$ and $\mathcal{B}_{ab} = -\frac{1}{2}u^c u^d \varepsilon_{ac}{}^{ef}\mathcal{W}_{efbd}$. The angle bracket means taking the trace-free part of a quantity.

Besides the above equations, it is useful to express the projected Ricci scalar $\hat{R}$ into the hypersurfaces orthogonal to u^a as

$$\hat{R} \doteq 2\kappa\rho - \frac{2}{3}\theta^2. \tag{15}$$

The spatial derivative of the projected Ricci scalar $\eta_a \equiv \frac{1}{2}a\hat{\nabla}_a \hat{R}$ is then given as

$$\eta_a = \kappa\hat{\nabla}_a \rho - \frac{2a}{3}\theta\hat{\nabla}_a \theta, \tag{16}$$

and its propagation equation by

$$\dot{\eta}_a + \frac{2\theta}{3}\eta_a = -\frac{2}{3}\theta a\hat{\nabla}_a \hat{\nabla}\cdot A - a\kappa\hat{\nabla}_a \hat{\nabla}\cdot q. \tag{17}$$

Finally, there are the conservation equations for the energy-momentum tensor

$$\dot{\rho} + (\rho + p)\theta + \hat{\nabla}^a q_a = 0, \tag{18}$$

$$\dot{q}_a + \tfrac{4}{3}\theta q_a + (\rho + p)A_a - \hat{\nabla}_a p + \hat{\nabla}^b \pi_{ab} = 0. \tag{19}$$

As we are considering a spatially flat universe, the spatial curvature must vanish on large scales and so $\hat{R} = 0$. Thus, from Eq. (15), we obtain

$$\tfrac{1}{3}\theta^2 = \kappa\rho. \tag{20}$$

This is the Friedmann equation in standard general relativity, and the other background equations (the Raychaudhuri equation and the energy-conservation equation) can be obtained by taking the zero-order parts of Eqs. (10) and (18), yielding

$$\dot{\theta} + \frac{1}{3}\theta^2 + \frac{\kappa}{2}(\rho + 3p) = 0, \tag{21}$$

$$\dot{\rho} + (\rho + p)\theta = 0. \tag{22}$$

All through this paper we only consider scalar perturbation modes, for which the vorticity ϖ_{ab} and magnetic part of Weyl tensor $\mathcal{B}_{ab}$ are at most of second order [59], and so are neglected in our first-order analysis.

B. Perturbation equations in k space

For the perturbation analysis it is more convenient to work in the k space, because we confine ourselves in the linear regime and different k modes decouple. Following [59], we shall make the following harmonic expansions of our perturbation variables

$$\hat{\nabla}_a\rho = \sum_k \frac{k}{a}\mathcal{X}Q_a^k \qquad \hat{\nabla}_a p = \sum_k \frac{k}{a}\mathcal{X}^p Q_a^k$$

$$q_a = \sum_k qQ_a^k \qquad \pi_{ab} = \sum_k \Pi Q_{ab}^k \qquad \hat{\nabla}_a\theta = \sum_k \frac{k^2}{a^2}\mathcal{Z}Q_a^k$$

$$\sigma_{ab} = \sum_k \frac{k}{a}\sigma Q_{ab}^k \qquad \hat{\nabla}_a a = \sum_k khQ_a^k \qquad A_a = \sum_k \frac{k}{a}AQ_a^k$$

$$\mathcal{E}_{ab} = -\sum_k \frac{k^2}{a^2}\phi Q_{ab}^k \qquad \eta_a = \sum_k \frac{k^3}{a^2}\eta Q_a^k \tag{23}$$

in which Q^k is the eigenfunction of the comoving spatial Laplacian $a^2\hat{\nabla}^2$ satisfying

$$\hat{\nabla}^2 Q^k = \frac{k^2}{a^2}Q^k$$

and Q_a^k, Q_{ab}^k are given by $Q_a^k = \frac{a}{k}\hat{\nabla}_a Q^k$, $Q_{ab}^k = \frac{a}{k}\hat{\nabla}_{\langle a}Q_{b\rangle}^k$.

In terms of the above harmonic expansion coefficients, Eqs. (6), (8), (11), (13), (16), and (17) can be rewritten as [59]

$$\tfrac{2}{3}k^2(\sigma - \mathcal{Z}) = \kappa q a^2, \tag{24}$$

$$k^3\phi = -\tfrac{1}{2}\kappa a^2[k(\Pi + \mathcal{X}) + 3\mathcal{H}q], \tag{25}$$

$$k(\sigma' + \mathcal{H}\sigma) = k^2(\phi + A) - \tfrac{1}{2}\kappa a^2\Pi, \tag{26}$$

$$k^2(\phi' + \mathcal{H}\phi) = \tfrac{1}{2}\kappa a^2[k(\rho + p)\sigma + kq - \Pi' - \mathcal{H}\Pi], \tag{27}$$

$$k^2\eta = \kappa\mathcal{X}a^2 - 2k\mathcal{H}\mathcal{Z}, \tag{28}$$

$$k\eta' = -\kappa q a^2 - 2k\mathcal{H}A, \tag{29}$$

where $\mathcal{H} = a'/a = \frac{1}{3}a\theta$, and a prime denotes the derivative with respect to the conformal time τ ($ad\tau = dt$). Also, Eq. (19) and the spatial derivative of Eq. (18) become

$$q' + 4\mathcal{H}q + (\rho + p)kA - k\mathcal{X}^p + \tfrac{2}{3}k\Pi = 0, \tag{30}$$

$$\mathcal{X}' + 3h'(\rho + p) + 3\mathcal{H}(\mathcal{X} + \mathcal{X}^p) + kq = 0. \tag{31}$$

C. The main equations

Recall that we are treating the modifications to GR as an EDM term and so include them in the (generalized) energy-momentum tensor T_{ab} to maintain the standard form of the Einstein equations. Thus, we can distinguish its different components $\rho_{\rm EDM}$, $p_{\rm EDM}$, $q_{a,\rm EDM}$, $\pi_{ab,\rm EDM}$ and their conservation. Depending on the specific model, the expressions for these components can be very different, but their conservation equations will take the same form. In particular, since the EDM has no coupling with standard model particles such as photons and baryons, it satisfies a separated conservation equation, Eqs. (30) and (31)

$$v'_{\rm EDM} + \mathcal{H}v_{\rm EDM} + kA - k\Delta_p + \tfrac{2}{3}k\Delta_\pi = 0, \tag{32}$$

$$\Delta'_{\rm EDM} + k\mathcal{Z} - 3\mathcal{H}A + 3\mathcal{H}\Delta_p + kv_{\rm EDM} = 0, \tag{33}$$

where we have defined the EDM peculiar velocity $v_{\rm EDM} \equiv q_{\rm EDM}/\rho_{\rm EDM}$, the density contrast $\Delta_{\rm EDM} \equiv \mathcal{X}_{\rm EDM}/\rho_{\rm EDM}$, and $\Delta_p \equiv \mathcal{X}^p_{\rm EDM}/\rho_{\rm EDM}$, $\Delta_\pi \equiv \Pi_{\rm EDM}/\rho_{\rm EDM}$ (c.f. Sec. II B) for the EDM, and used the fact that $p_{\rm EDM} = 0$ to reproduce the standard CDM background evolution. The prime here is the derivative with respect to the conformal time and $\mathcal{H} = a'/a$.

On the other hand, the spatial derivative of Eq. (10) gives the evolution equation for $\mathcal{Z}$ as

$$k'\mathcal{Z} + k\mathcal{H}\mathcal{Z} - kA + \tfrac{1}{2}\kappa(\mathcal{X} + 3\mathcal{X}^p)a^2 = 0 \tag{34}$$

and in this equation $\mathcal{X}$, $\mathcal{X}^p$ are, respectively, the density and pressure perturbations for *all* the matter species, including the EDM. For convenience, we shall work in the frame where $A = 0$. In this case, if the Universe is dominated by the EDM, then the three equations above can be combined to eliminate $\mathcal{Z}$ and $v_{\rm EDM}$

$$\Delta''_{\rm EDM} + \mathcal{H}\Delta_{\rm EDM} - \tfrac{1}{2}\kappa\rho_{\rm EDM}a^2\Delta_{\rm EDM} - \tfrac{2}{3}k^2\Delta_\pi + 3\mathcal{H}\Delta'_p + \left[3\mathcal{H}' + 3\mathcal{H}^2 - \tfrac{3}{2}\kappa\rho_{\rm EDM}a^2 + k^2\right]\Delta_p = 0. \tag{35}$$

If other matter species could not be neglected, as is in the radiation-dominated era and early-matter era, then we only need to correct the above equation by adding to it $\frac{1}{2}\kappa\rho_{\rm EDM}a^2\Delta_{\rm EDM}$ another term with $\frac{1}{2}\kappa\rho_b a^2\Delta_b + \kappa\rho_r a^2\Delta_r$ (where ρ_b, ρ_r are the baryon and radiation energy densities), which comes from the last term in the left-hand side of Eq. (34), and these new terms do not affect the qualitative features of our discussion (we will include them in the numerical calculation). Equation (35) tells us that the evolution of the density perturbation in EDM is completely controlled by its stress history: the EDM equation of state $w_{\rm EDM} = p_{\rm EDM}/\rho_{\rm EDM}$ controls the background expansion and is set to zero here; the other two stress variables Δ_p, Δ_π then drive the evolution of $\Delta_{\rm EDM}$ through Eq. (35). Note that the stresses of the EDM are external functions determined by microphysics (for particle dark matter) or a particular modified gravity theory, and must be specified to close the system of Einstein equations and conservation equations. In the special case where $\Delta_p = \Delta_\pi = 0$, we reduce to the CDM model for which $\Delta_{\rm CDM} \propto a$ in the matter era; but in general, there will be deviations from this growing solution.

Next, we look at the evolution of the gravitational potential ϕ (see Secs. II A and II B). By manipulating Eqs. (25)–(27) and (30), and working again in the $A = 0$ frame, we can eliminate the terms involving q and obtain the following evolution equation

$$\phi'' + 3\mathcal{H}\left(1+\frac{p'}{\rho'}\right)\phi' + \left[2\mathcal{H}' + \mathcal{H}^2\left(1+3\frac{p'}{\rho'}\right)\right]\phi + k^2\frac{p'}{\rho'}\phi$$
$$= \frac{1}{2}\kappa\rho a^2\left(\Delta_p - \frac{p'}{\rho'}\Delta\right) - \frac{1}{2k^2}\kappa\rho a^2\Delta_\pi'' - \frac{1}{2k^2}\kappa\rho a^2$$
$$\times\left[\left(5+3\frac{p'}{\rho'}\right)\mathcal{H} + 2\frac{\rho'}{\rho}\right]\Delta_\pi' - \frac{1}{2k^2}\kappa\rho a^2$$
$$\times\left[\left(5+3\frac{p'}{\rho'}\right)\left(\mathcal{H}+\frac{\rho'}{\rho}\right)\mathcal{H} + \frac{\rho''}{\rho} + \left(\frac{2}{3}+\frac{p'}{\rho'}\right)k^2\right]\Delta_\pi, \tag{36}$$

where ρ, p are the total energy density and total pressure, respectively, and $\rho \equiv \rho_{\rm EDM}$, with $p = 0$ for an EDM dominated universe. The term $\frac{1}{2}\kappa\rho a^2(\Delta_p - \frac{p'}{\rho'}\Delta)$ is zero for radiation and baryons, but in general could be nonzero for the EDM. Again, we see that the stress history of the EDM completely specifies the evolution of ϕ. As we shall see in what follows, the dark-matter component influences the CMB power spectrum through the gravitational potential, and so the stress history of the EDM is of crucial importance for the CMB.

In summary, we have seen that the properties of the (isotropic and anisotropic) stresses of the EDM determine the evolution of the matter density perturbation and the gravitational potential, and thereby determine the predicted matter power spectrum (through the former) and the CMB spectrum (through the latter) [60]. As we discussed in Sec. I, the predicted matter power spectrum of a theory records the matter energy density perturbation at a specific time—today, and it is easier to make it consistent with observations, as evident from the studies of TeVeS and $f(K)$ theories. Thus, in this work we shall start from an EDM theory that is constructed already to predict an acceptable matter power spectrum; that is, we fix the matter energy density perturbation today and calculate the influence of different δ_m evolution paths on the CMB spectrum. In this way, we can reduce our model space to one that is of realistic interests.

III. THE DARK-MATTER EFFECTS ON CMB

It is helpful to have a brief review of the CMB physics and how it is affected by dark matter before we go into the numerics to show the effects of EDM stresses on the CMB. Here, we will just present a minimal description of this topic; for more details see the reviews [61–64].

The primary CMB spectrum is determined by inhomogeneities in the CMB photon temperature at the time of recombination. Prior to the recombination, photons couple tightly by Thomson scattering with electrons, which themselves couple to baryons via Coulomb interaction; thus to a first approximation photons and baryons combine into a single fluid. Dark matter, on the other hand, does not couple electromagnetically, but only interacts through gravitational effects and so contributes to the gravitational potential in which the baryon-photon fluid moves.

When the density perturbation in the photons grows, hot (cold) spots appear where the local photon density is higher (lower) than average. The higher photon density means higher pressure, which will tend to counteract the growth of local photon density. This will lead to acoustic oscillations of the gauge invariant photon temperature perturbation Θ, which is also a characterization of the photon number density perturbation. In reality, this picture becomes a bit more complicated because of the interplay between baryons and dark matter: baryons couple tightly to photons, and move with them so that the inertia of the fluid is increased, while the gravitational potential produced by dark matter drives the oscillations. More specifically, if we use the multipole decomposition

$$\Theta = \sum_\ell (-i)^\ell \Theta_\ell P_\ell(\mu),$$

where P_ℓ is the Legendre function and $k\mu = \mathbf{k}\cdot\gamma$ with γ being the direction of photon momentum, then in the tight-coupling limit the monopole Θ_0 satisfies a driven-oscillator equation [65]

$$\Theta_0'' + \frac{R}{1+R}\mathcal{H}\Theta_0' + k^2 c_s^2\Theta_0 = F, \tag{37}$$

in which

$$F = -\Phi'' - \frac{R}{1+R}\mathcal{H}\Phi' - \frac{1}{3}k^2\Psi, \tag{38}$$

where

$$R \equiv 3\rho_b/4\rho_\gamma, \qquad c_s^2 \equiv 1/3(1+R)$$

and

$$\Psi = \phi - \frac{1}{2}\frac{a^2}{k^2}\kappa\Pi, \qquad \Phi = -\phi - \frac{1}{2}\frac{a^2}{k^2}\kappa\Pi$$

are, respectively, the (frame-independent) Newtonian potential and curvature perturbations. The dipole moment Θ_1, which equals the peculiar velocity of baryons thanks to the tight coupling, satisfies $k\Theta_1 + 3\mathcal{H}\Theta_0' + 3\Phi' = 0$, and all higher moments $\Theta_\ell(\ell \geq 2)$ vanish because the frequent scattering makes the photon distribution isotropic in the electron rest frame.

Thus, on large scales the photon temperature perturbation displays a pattern of driven and damped oscillation. On scales smaller than the photon mean free path, which itself grows in time, however, the tight coupling approximation is no longer perfect and quadrupole moments of the temperature perturbation needs to be taken into account. This introduces a dissipation term into the oscillator equation above, which damps the oscillations.

At the time of recombination, the number density of free electrons drops suddenly, and there ceases to be coupling between baryons and photons. The CMB photons then free

stream toward us. This free-streaming solution is given by [65]

$$\Theta_\ell(\tau_0) \approx (\Theta_0 + \Psi)(\tau_*)(2\ell + 1)j_\ell(k\Delta\tau_*) + \Theta_1(\tau_*)[\ell j_{\ell-1}(k\Delta\tau_*) - (\ell + 1)j_{\ell+1}(k\Delta\tau_*)] + (2\ell + 1)\int_{\tau_*}^{\tau_0}(\Psi' - \Phi')j_\ell[k(\tau_0 - \tau)]d\tau, \quad (39)$$

where τ_0, τ_* are the conformal times today and at recombination, $\Delta\tau_* = \tau_0 - \tau_*$ and $j_\ell(x)$ is the spherical Bessel function of order ℓ. The terms $\Theta_0 + \Psi$ and Θ_1 are, respectively, the monopole and dipole moments of the CMB temperature field at τ_*, and can be calculated using the equations above (a Ψ is added to Θ_0, which accounts for the redshift in the photon energy, and thus temperature, when it climbs out of the Newtonian potential). Finally, the CMB temperature-temperature spectrum is defined as

$$\frac{2\ell + 1}{4\pi}C_\ell = \frac{V}{2\pi^2}\int\frac{k^3|\Theta_\ell(\tau_0, k)|^2}{2\ell + 1}d\ln k. \quad (40)$$

These are the leading-order effects in the CMB physics, and we could see how they affect the CMB power spectrum. Because $j_\ell(x)$ peaks strongly at $\ell \sim x$, so perturbations on very large scales (small k) mainly affect the low-ℓ spectrum. If the Universe is completely dominated by matter at τ_*, then the first term in Eq. (39) is given by $(\Theta_0 + \Psi)(\tau_*) \approx \Psi(\tau_*)/3$, and accounts for the ordinary Sachs-Wolfe effect; meanwhile, if the potential $\Psi - \Phi = 2\phi$ decays between τ_* and τ_0, then the integration in Eq. (39) will also make a significant contribution as photons travel in and out of many time-dependent potentials along the line of sight, and this is the integrated Sachs-Wolfe (ISW) effect.

Going to higher ℓ one can see the peak structures of the CMB spectrum. The peaks appear since at τ_*, when the oscillating pattern of Θ_0 [c.f. Eq. (37)] freezes, Θ_0 might be just at its extrema for some scales (k); and these extrema are then converted to extrema of C_ℓ through Eqs. (39) and (40). Since what appears in Eq. (40) is $|\Theta_\ell|^2$, both the maxima and minima of $(\Theta_0 + \Psi)(\tau_*)$ will appear as peaks in C_ℓ. If there are no baryons and the potential Ψ is constant, then the even and odd peaks should be of the same amplitude. The inclusion of baryons effectively increases the inertia of the baryon-photon fluid and displaces the balance point of $\Theta_0 + \Psi$, and as a result, after taking $|\cdots|^2$, the odd and even peaks appear to have different heights. At the same time, from Eqs. (39) and (40), we see that the dipole $\Theta_1(\tau_*)$ also contributes to C_ℓ through modulation. But Eq. (39) shows that its power is more broadly distributed, and so its contribution is significantly smaller than that of the monopole. Where the monopole vanishes the dipole becomes important and this is why the troughs of C_ℓ are of nonzero amplitude.

If one goes to still higher ℓ, there are two effects. First, the higher ℓ moments mainly receive contributions from the small-scale (large k) perturbations, which began oscillating already during the radiation-dominated era (not much earlier than τ_*). Since in the radiation era the potential Φ decays, this decay will drive the monopole oscillation through the source term in Eq. (37) and lead to an increase in the oscillation amplitudes. This explains why in some models the third peak is higher than the second. Second, as discussed above, on very small scales there is severe damping of the oscillations because of photon diffusion. The combination of these two effects causes the CMB power in ℓs higher than the third peak to be significantly damped.

We can now highlight the key places where the dark-matter effects enter CMB physics through the gravitational potential it produces and contrast the situation with that when EDM is employed as a substitute. First, if CDM is replaced by EDM, then in the analysis of Sec. II the time evolutions of ϕ, and thus of Φ and Ψ are modified. If the modification only becomes significant after τ_*, the ISW effect could be different from standard CDM (where it effectively vanishes). If it differs from standard CDM before τ_*, then the Sachs-Wolfe effect will be altered as well. Second, the deviation of Φ and Ψ from their values in standard CDM before τ_* can change the zero point of the monopole oscillation through baryon loading, thereby modifying the relative heights of the odd and even peaks. Third, the modification of Φ and Ψ also changes the driving force in Eq. (37), and results in different amplitudes for the C_ℓ at high ℓ. In Sec. IV, we shall give some numerical examples showing these effects explicitly in our EDM model.

IV. NUMERICAL EXAMPLES

In this section, we turn to some numerical examples to illustrate the qualitative analysis of Sec. III. As mentioned in Sec. II, we choose to fix the endpoint of the evolution of the matter energy density perturbation. This gives us a freedom to parametrize the evolution of $\Delta_{\rm EDM}(a)$, which is generally different from that of $\Delta_{\rm CDM}(a) \propto a$ (in matter regime). Once the $\Delta_{\rm EDM}$ parametrization is given (or in other words the model is set up), Eq. (35) becomes an evolution equation for Δ_p and Δ_π. This is insufficient to solve for Δ_p and Δ_π, so in the following numerical calculations we consider three cases: (1) $\Delta_\pi = 0$, (2) $\Delta_p = 0$, and (3) a more realistic case where both Δ_p and Δ_π are nonzero. Since any scale dependence of $\Delta_{\rm EDM}$ will alter the shape of the matter power spectrum, and thus incur stringent constraints, we parametrize $\Delta_{\rm EDM}(a)$ so that it is independent of k.

A. The case of $\Delta_\pi = 0$

When $\Delta_\pi = 0$ and $\Delta_{\rm EDM}$ is specified, Eq. (35) becomes a first-order evolution equation for Δ_p

$$3\mathcal{H}\Delta_p' + \left[3\mathcal{H}' + 3\mathcal{H}^2 - \frac{3}{2}\kappa\rho_{\rm EDM}a^2 + k^2\right]\Delta_p = S, \tag{41}$$

where the source term S is given by[1]

$$S = -\Delta_{\rm EDM}'' - \mathcal{H}\Delta_{\rm EDM}' + \frac{1}{2}\kappa\rho_{\rm EDM}a^2\Delta_{\rm EDM} + \frac{1}{2}\kappa\rho_b a^2\Delta_b + \kappa\rho_r a^2\Delta_r. \tag{42}$$

The quantity Δ_p does not appear directly in the expression for gravitational potential [c.f. Eqs. (25) and (27)]; however, it does affect the potential ϕ *indirectly* through the evolution of $v_{\rm EDM}$ Eq. (32). Consequently, there are now two new variables (Δ_p and $v_{\rm EDM}$) to evolve in the model, and we need to specify their initial conditions.

Here, we adopt the simplest and most direct approach, namely, to assume that the EDM evolves as CDM prior to some initial time τ_i, when the scale factor is a_i and the dark-matter density perturbation Δ_i, and for $a > a_i$ the dark-matter density perturbation begins to evolve as $\Delta_{\rm EDM}(a)$. This means that for $a < a_i$ the variables Δ_p and $v_{\rm EDM}$[2] will remain zero: this provides the desired initial conditions. This simple approach captures most of the interesting features about EDM. However, by assuming that at early times EDM is just CDM, we cannot account for more complicated issues such as the primordial power spectrum, and we will comment on this in the concluding section.

Now, we could turn to a specific example of $\Delta_{\rm EDM}(a)$ parametrization. We let $\Delta_{\rm EDM}(a)$ equal $\Delta_{\rm CDM}(a)$ in the standard CDM model at times a_i and a_f, and assume that the deviation from standard CDM occurs between a_i and a_f. Here, $a_f \le a_0$ and $a_0 = 1$ is the current time. In order to characterize the deviation from standard CDM between a_i and a_f, we introduce a parameter b to denote the ratio of $\Delta_{\rm EDM}$ to $\Delta_{\rm CDM}$ at the mean time $a = (a_i + a_f)/2$. Since for standard CDM we have $\Delta_{\rm CDM}(a) \propto a$, the parametrized $\Delta_{\rm EDM}$ is simply a parabola, which passes through three points (a_i, Δ_i), $(a_f, \Delta_i a_f/a_i)$, and $(\frac{a_i+a_f}{2}, b\frac{\Delta_i}{a_i}\frac{a_i+a_f}{2})$ between times when the scale factor lies between a_i and a_f

$$\Delta_{\rm EDM}(a) = \frac{\Delta_i}{a_i}a - 2\frac{\Delta_i}{a_i}\frac{a_f + a_i}{(a_f - a_i)^2}(b-1)(a - a_i) \times (a - a_f) \tag{43}$$

for $a \in [a_i, a_f]$. Some examples of $\Delta_{\rm EDM}(a)$ with different choices of b are shown in Fig. 1. It clearly shows that b characterizes the deviation from a standard CDM evolution ($b = 0$). Note that the parametrization Eq. (43) is just an example for illustration, and specific modified gravity models like TeVeS and $f(K)$ theory may lead to different parametrization, which however can similarly be tested.

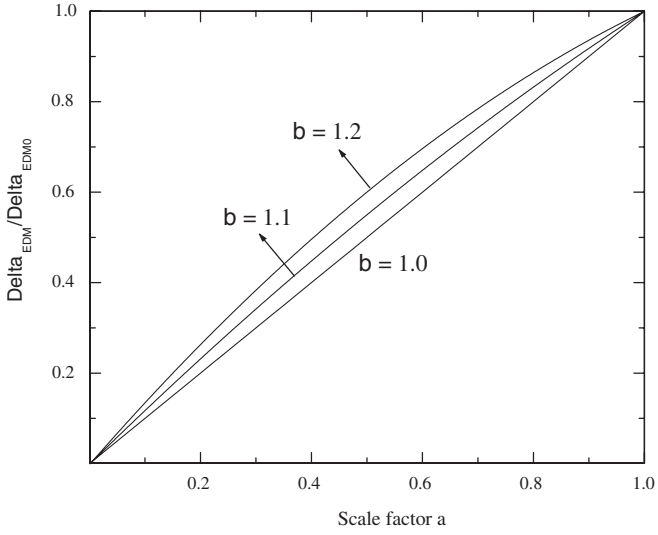

FIG. 1. Some example parameterizations for the evolution of $\Delta_{\rm EDM}$, normalized to its current value $\Delta_{\rm EDM0}$, as described in Eq. (43). The values of the parameter b are indicated; the other parameters are $a_i = 0.005$ and $a_f = 1$.

Then with the parametrization of $\Delta_{\rm EDM}(a)$ in Eq. (43), we could numerically evolve the relevant perturbation equations and see the changes in the CMB power spectrum. First, we assume $\tau_i > \tau_*$. In this situation the CMB physics prior to last scattering is unaffected and so from Eq. (39) we see that only the integration is modified. This is because in the standard CDM model the gravitational potential $\phi = (\Psi - \Phi)/2$ remains constant during the matter epoch, and the integrand in Eq. (39) vanishes. For the present EDM case, however, Eq. (36) dictates that $\phi' \neq 0$ even in the matter era; consequently, there will be a significant ISW effect to boost the low-ℓ CMB power. As shown in Fig. 2, the earlier the EDM evolution deviates from that of CDM (i.e., the smaller a_i is), the earlier ϕ begins to evolve and the larger the cumulative ISW effect is.

Next, we consider the case where the deviation from CDM evolution begins earlier than last scattering. In this case the evolution of $\Delta_{\rm EDM}$ and thus the potential ϕ is changed before last scattering, and correspondingly the first two terms in Eq. (39) are modified as well. In Fig. 3, we have displayed the primary CMB power spectrum for the $\Delta_{\rm EDM}(a)$ parametrization Eq. (43) with parameters $a_i = 0.0002$, $a_f = 0.002$,[3] $b = 1.2$, 1.0, 0.8, and the ISW effect switched off for simplicity. A larger value of b implies a larger EDM density perturbation (for the scales

[1]Here, we include the effects of baryons and radiation explicitly.

[2]Recall that we work in the $A = 0$ frame, in which $v_{\rm CDM} = 0$.

[3]Note that in reality the Universe is not completely matter dominated between $a = 0.0002$ and $a = 0.002$, and as a result the parametrization Eq. (43), with $b = 1$, is not exactly the same as $\Delta_{\rm CDM}(a)$. The qualitative features, however, are not affected by this small deviation.

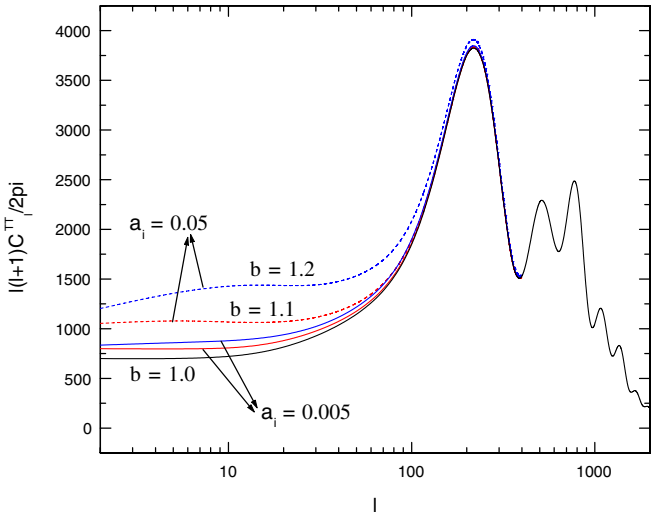

FIG. 2 (color online). (color online) The CMB power spectrum for our $\Delta_\pi = 0$ model with $\Delta_{\rm EDM}(a)$ parameterized as in Eq. (43). Three values of b are adopted: $b = 1.2$ (blue curves), $b = 1.1$ (red curves), and $b = 1.0$ (black curve). The dashed curves are the cases where $a_i = 0.005$ and the solid colored ones $a_i = 0.05$. For all the curves we set $a_f = 1.0$.

relevant to the first acoustic peak) before the last scattering and therefore a deeper Newtonian potential Ψ. This means that the CMB photons experience larger redshifts when climbing out of the potential after last scattering, and the effective temperature $(\Theta_0 + \Psi)(\tau_*)$ is lower, leading to a suppressed first CMB acoustic peak. When b is smaller the opposite effect occurs (c.f. Fig. 3). At the higher-ℓ peaks this effect is less significant because the potential for the relevant (smaller) scales has already decayed. However, as

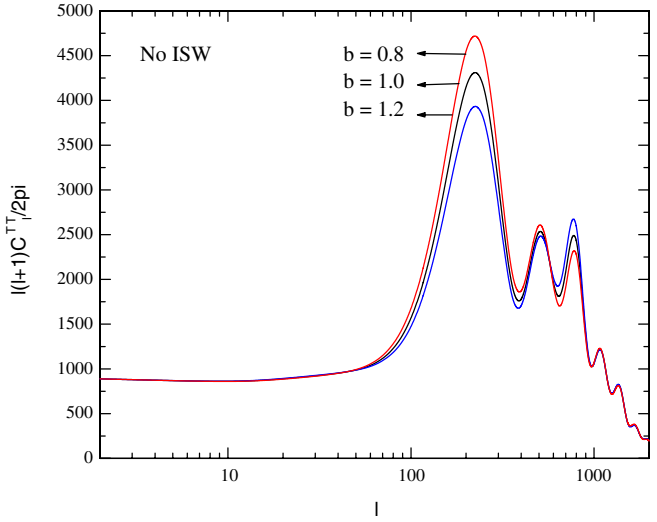

FIG. 3 (color online). (color online) The primary CMB spectrum with the ISW contribution removed, for the parameters $a_i = 0.0002$, $a_f = 0.002$ and $b = 1.2$ (blue curve), 1.0 (black curve) and 0.8 (red curve), respectively.

discussed in Sec. III, the change in the potential prior to last scattering also modifies the equilibrium point of the monopole oscillation and alters the relative heights of odd and even CMB peaks. If Ψ is a constant, the difference between odd and even peaks in $|\Theta_0 + \Psi|$ is proportional to $|\Psi|$ [62], so increasing b amplifies this difference by increasing Ψ, and as shown in Fig. 3, the third peak becomes higher and the second peak becomes lower for larger values of b and go oppositely for smaller b. In this figure, the fourth peak and onwards are not affected significantly because our parameters are chosen conservatively. There, however, *could* be alternative dark-matter models where the higher peaks also deviate from the CDM predictions, for an example see Fig. 4 (upper panel) of [41].

The CMB power spectrum has been measured to high precision by many experiments (see for example [66,67]) and will be further improved in the future, so it could be used to constrain the EDM model here. For higher ℓs the CMB data could be used directly. For lower ℓs its usability is limited by the cosmic variance. If the deviation is significant (such as those in Fig. 2), then we could use CMB data alone to constrain the model, as in [68]. Otherwise, we could cross correlate the observed ISW with the matter density perturbation observable [69]; because both are modified in the EDM model, we should expect different correlations from those created by CDM. Actually, this technique has been applied to TeVeS [70] but may not serve as a perfect EDM discriminator because there will be contaminations from the dark-energy component in the galaxy-CMB correlation. Meanwhile, the general EDM model has different gravitational potential, matter density perturbation, as well as a possible different redshift distribution of lensing galaxies, and these will also change the weak lensing spectrum (see [71] for an application to one modified dark-matter model). Finally, the different evolution history of $\Delta_{\rm EDM}(a)$ may also have implications for the formation of nonlinear structure. These further possibilities are beyond the scope of this work and will be further pursued elsewhere.

B. The case of $\Delta_p = 0$

In the case of $\Delta_p = 0$, Eq. (35) simply becomes an algebraic equation for Δ_π

$$\frac{2}{3}k^2\Delta_\pi = \Delta''_{\rm EDM} + \mathcal{H}\Delta'_{\rm EDM} - \frac{1}{2}\kappa\rho_{\rm EDM}a^2\Delta_{\rm EDM} - \frac{1}{2}\kappa\rho_b a^2\Delta_b - \kappa\rho_r a^2\Delta_r. \quad (44)$$

For the parametrization of $\Delta_{\rm EDM}(a)$ we will still use Eq. (43). In this case, because Eq. (44) is algebraic, the only variable to propagate in time is $v_{\rm EDM}$ [c.f. Eq. (32)], and as in Sec. IV A we could take $v_{\rm EDM} = 0$ prior to a_i and then evolve it using Eq. (32) for $a > a_i$.

In Fig. 4 we have plotted the CMB spectrum for such a model with $b = 1.001$ and different choices of a_i, from

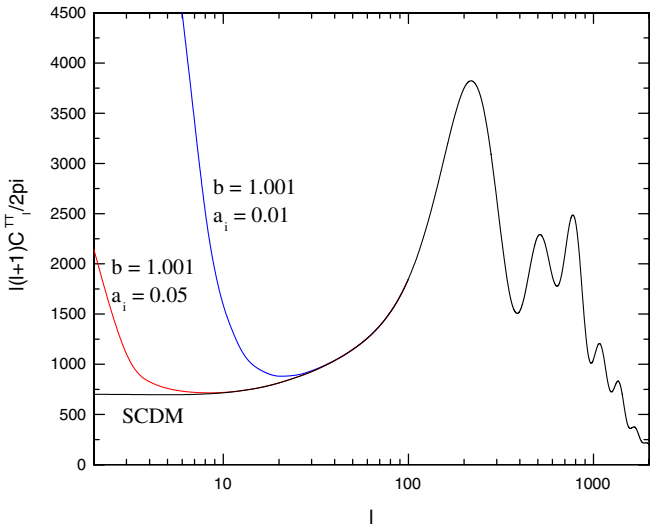

FIG. 4 (color online). (color online) The CMB spectrum of the model $\Delta_p = 0$ with the $\Delta_{\rm EDM}(a)$ parametrization given in Eq. (43) and parameters $a_i = 0.01$ (blue curve) and $a_i = 0.05$ (red curve), respectively. The black curve is the SCDM model. The other parameters are $b = 1.001$ and $a_f = 1.0$.

which we can see that the low-ℓ CMB power is very sensitive to both b and a_i. The reason is that, although the right-hand side of Eq. (44) is scale independent thanks to our parametrization Eq. (43), its left-hand side *is* scale-dependent through the k^2 factor. Consequently, on large scales (small k) the EDM anisotropic stress Δ_π could be very large, and so the gravitational potential ϕ is significantly different than that in standard CDM [c.f. Eq. (25)]. The late ISW effect is then modified, which enhances the low-ℓ CMB power. On smaller scales, Δ_π is suppressed by k^{-2}, and its effects soon becomes negligible, explaining why the high-ℓ CMB power is not influenced. Also, the smaller a_i is, so the earlier the CMB evolution of the $\Delta_p = 0$ EDM model deviates from the standard CDM result. Note that, in the case of standard CDM, the right-hand side of Eq. (44) vanishes identically, and so there is no influence on the last ISW.

It is then clear that the $\Delta_p = 0$ EDM model with a general scale-independent parametrization of $\Delta_{\rm EDM}(a)$ is problematic and already stringently constrained. A possible way out of this trouble is to drop the scale independence of $\Delta_{\rm EDM}(a)$. We have numerically checked that if on large scales $\Delta_{\rm EDM}$ grows as $\Delta_{\rm CDM}$, then the low ℓ boosts of the CMB power as shown in Fig. 4 disappear, and one recaptures the standard CDM results of ISW effect. Another possibility is to have both Δ_π and $\Delta_{\rm EDM}(a)$ scale independent and also include Δ_p; this will be considered in Sec. IV C.

C. General Δ_p and Δ_π

If the EDM arises from modifications to standard general relativity, then in general neither Δ_p nor Δ_π would be exactly zero. In this case, there are many more possibilities because Δ_p and Δ_π cannot be uniquely solved from Eq. (35). Of course, the evolution of ϕ might also be modified normally, and this could be used to constrain Δ_p and Δ_π. Indeed, we could use the freedom to choose Δ_p and Δ_π so that the evolution of ϕ [c.f. Eq. (36)] is exactly (or nearly) the same as that in standard CDM. Let us consider such an example now.

In order that the gravitational potential evolves in the same way as in standard CDM, we require the contribution on the right-hand side of Eq. (36) from the EDM to vanish, which leads to the following evolution equation for Δ_π

$$\Delta_\pi'' - \frac{3\rho_m}{4\rho_r + 3\rho_m}\mathcal{H}\Delta_\pi' + \left[\frac{4\rho_r + 2\rho_m}{4\rho_r + 3\rho_m}k^2 - 3\mathcal{H}' - \frac{12\rho_r + 3\rho_m}{4\rho_r + 3\rho_m}\mathcal{H}^2\right]\Delta_\pi = k^2\Delta_p, \tag{45}$$

where ρ_m and ρ_r are, respectively, the energy densities of nonrelativistic (baryons plus EDM) and relativistic (photons plus neutrinos) matter. Here, note that the time evolution of Δ_π is driven by Δ_p, which itself evolves in accord with Eq. (35), which is driven by Δ_π *plus* the *parametrized* $\Delta_{\rm EDM}(a)$ (with its time derivatives). So, in the numerical calculation we have four more variables to propagate: Δ_p, $v_{\rm EDM}$, Δ_π, and Δ_π'.

Note that if Δ_p vanishes identically and $\Delta_\pi = 0$ initially, then Δ_π will remain zero all the time; also, if Δ_π vanishes identically, then so does Δ_p. These restrictions indicate that the two cases we have considered in the above subsections *cannot* give rise to the same evolution of ϕ *and* different evolution of $\Delta_{\rm EDM}$ to that predicted by standard CDM at the same time. The general case with $\Delta_p, \Delta_\pi \neq 0$, however, is able to do this, as is shown in Fig. 5. There, we plot the CMB power spectra of this general case with different values of $b = 1.1,\ 1.0,\ 0.9$, respectively, and they are totally indistinguishable because the evolutions of ϕ are identical, leading to identical (zero) ISW effects. In this figure, we have chosen $a_i = 0.005$ and $a_f = 1$ so that we only require the EDM to deviate from CDM after last scattering. It must be emphasized that, although the three curves are indistinguishable from each other, they *do* correspond to different EDM properties. To show this point clearly, we display in Fig. 6 the quantities $c_s^2 \equiv \Delta_p/\Delta_{\rm EDM}$ and $c_v^2 \equiv \Delta_\pi/\Delta_{\rm EDM}$, which characterize the importance of Δ_p and of Δ_π, respectively, for the models. It is obvious that in the $b \neq 1$ models these quantities could be very different from the standard CDM value (0), and this can be understood intuitively as follows: the pressure perturbation term Δ_p acts *against* gravitational collapse, when $b > 1$, meaning that $\Delta_{\rm EDM}$ grows faster than $\Delta_{\rm CDM}$ early on and more slowly later; Δ_p needs to be negative early on and positive later (and vice versa). The anisotropic stress term Δ_π dissipates fluctuations in $\Delta_{\rm EDM}$ [c.f. Eq. (35)] and behaves similarly in the figure.

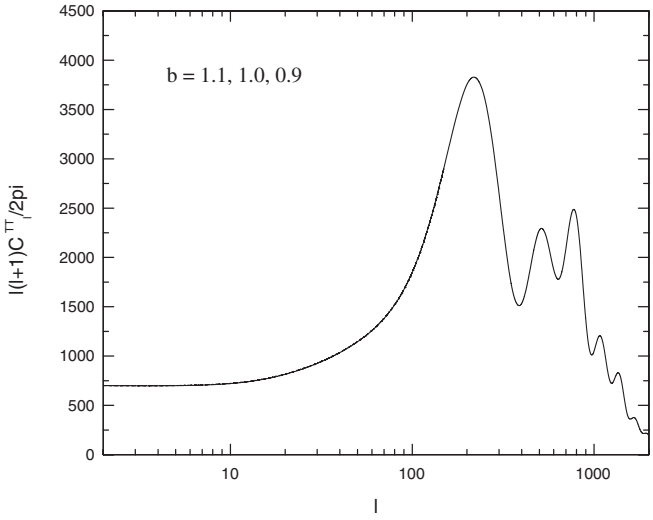

FIG. 5. The CMB power spectrum for the model in which $\Delta_{\rm EDM}(a)$ is parameterized as Eq. (43), both Δ_p and Δ_π are nonzero and satisfy a relation as described in the text. The solid, dashed and dotted curves represent the cases of $b = 1.0, 1.1, 0.9$, respectively, and they cannot be distinguished in the figure because they experience identical gravitational potential evolution. The other parameters are $a_i = 0.005$ and $a_f = 1$.

We have thus seen that the observations of the CMB and matter power spectrum *cannot* rule out this general case (as long as a_i is after last scattering). Cross correlating ISW with the galaxy distribution might help in this regard, but it is still limited for two reasons: first, it is contaminated by the effects of dark energy, and second, the cross-correlation data only exists for late times and cannot effectively constrain models like ours where the deviation from CDM occurs much earlier.

If we choose the $a_i \lesssim 10^{-3}$, which means that the deviation of EDM from CDM starts before last scattering, then although Eq. (45) guarantees that the ϕ evolution is not changed for arbitrary b, the CMB power spectrum will generally be different from that of standard CDM because the quantities Φ and Ψ, which are directly relevant for the primary CMB anisotropy, are modified since $\Phi = -\phi - \frac{\kappa\Pi a^2}{2k^2}$, $\Psi = \phi - \frac{\kappa\Pi a^2}{2k^2}$. In Fig. 7, we present such an example, for which we have used the parametrization Eq. (43) of $\Delta_{\rm EDM}(a)$ with $a_i = 0.0002$ and $a_f = 0.002$. This shows that in general the small-angle (high-ℓ) CMB power will be different even though the large-angle power is fixed to be the same as in standard CDM. If the evolution of $\Delta_{\rm EDM}$ prior to last scattering is significantly different from that of CDM, then the deviation of CMB spectrum might be very large, and this is why the CMB could efficiently constrain such alternative gravitational dark-matter theories as TeVeS and the $f(K)$ models.

Another possible constraint comes from the CMB polarization. The linear polarization of CMB photons carries information about the gravitational potential because it can only be generated from the quadrupole moment of the CMB temperature perturbation, which is related to the anisotropic photon stress [72,73], through Thomson scat-

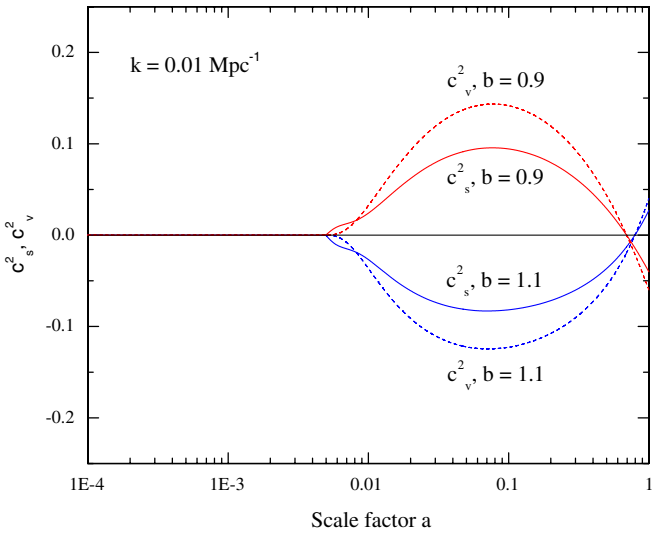

FIG. 6 (color online). (color online) The quantities $c_s^2 \equiv \Delta_p/\Delta_{\rm EDM}$ (solid curves) and $c_v^2 \equiv \Delta_\pi/\Delta_{\rm EDM}$ (dashed curves) as functions of a. The black line is for SCDM ($c_s^2 = c_v^2 = 0$), and the red/blue lines are for the model described in the text with $b = 0.9$, 1.1, respectively. All curves are for the scale $k = 0.01$ Mpc^{-1}.

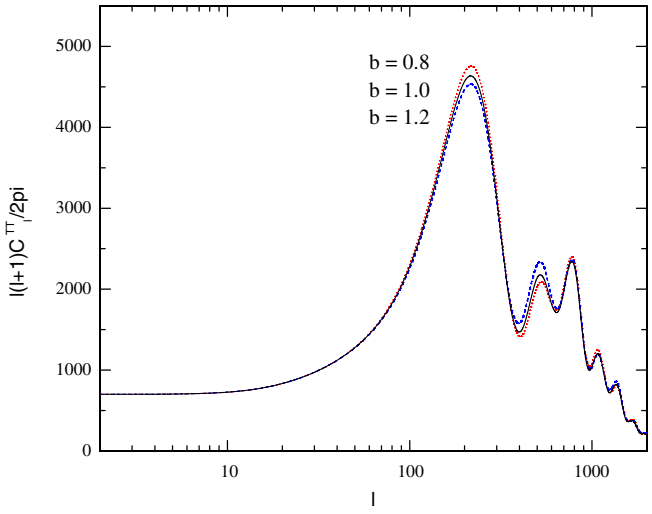

FIG. 7 (color online). (color online) The CMB spectrum for the general case [c.f. Eq. (45)] with $\Delta_{\rm EDM}(a)$ parameterized as in Eq. (43). Here, we have chosen $a_i = 0.0002$ and $a_f = 0.002$. The blue dashed, black solid, and red dotted curves represent the cases for $b = 1.2$, 1.0, and 0.8, respectively, as also shown beside the curves. The large-angle ($\ell < 100$) CMB powers are indistinguishable for the curves as in Fig. 5 due to the identical evolutions of ϕ and identical ISW effects.

tering. Furthermore, at earlier times the rapid scattering of photons by electrons ruins the photon anisotropic stress (c.f. Sec. III); consequently, the polarization only appear close to last scattering when significant photon quadrupole anisotropy can be produced. The localization of the generation in time, and the dependence on the quadrupole moment, only mean that the polarization directly reflects the gravitational potentials at the time of last scattering in a special way and so provides invaluable information about the EDM. This is in contrast to the CMB temperature spectrum, which depends on the gravitational potentials through the entire cosmic history up to now, and also on the photon monopole and dipole moments, which complicate the extraction of information. In Fig. 8, we plot the CMB EE polarization and TE cross-correlation spectrum for the same model as in Fig. 7. It can be seen that different parameters give quite distinct peak features. The CMB polarization was first detected in 2002 [74], with the precision gradually improved since then [75]. Although the precision at present is still insufficient to place stringent constraints on the EDM model, we expect that future observations will change this situation.

We could also slightly change Eq. (45) to make the evolution of Φ *or* Ψ the same as that for standard CDM, however, clearly this is not possible for *both* Φ *and* Ψ because in this case $\Delta_\pi \neq 0$. Because the primary CMB anisotropy is determined by both of these two variables, it will almost definitely differ between the EDM and CDM models. Furthermore, in the most general cases the evolution of ϕ will be changed as well, which gives rise to different low-ℓ CMB spectra. Therefore, we expect that the CMB data will place stringent constraints on the general EDM models, and can be used to distinguish alternative gravitational theories of dark matter. Conversely, any attempt of modification of general relativity, which claims to have reproduced the observed large-scale structure, must be confronted with the CMB fluctuation spectrum and polarization to test its viability.

V. SUMMARY AND DISCUSSION

Motivated by the recent developments in producing the large-scale structure formation with alternative theories of gravity, we have considered the prospect of using the CMB to constrain such theories in new ways. We take the confrontation with the matter power spectrum data as a first test of the perturbed cosmological model in our alternative gravity theory and assume that this test has been passed. This is because the currently successful theories like TeVeS and $f(K)$ really are *only* able to reproduce the observed LSS rather than all the perturbation observables, and such a simplifying assumption efficiently restricts our model space so that the degeneracy problem is somewhat alleviated. As discussed in Sec. II, reproducing the observed LSS is a rather weak requirement on the theory because the LSS only reflects the density perturbations at late time. This means that there is still considerable freedom to choose the evolution history of the dark-matter density perturbation $\Delta_{\rm EDM}$, which will generally lead to different predictions about other cosmological observables such as the CMB spectra and polarization.

We discussed how this freedom in the evolution history can be utilized by considering an example of the parametrization [c.f. Eq. (43)] of $\Delta_{\rm EDM}(a)$, which only reduces to the familiar $\Delta_{\rm CDM}(a)$ result with the parameter choice $b = 1.0$. As was shown in Sec. II, the evolution of $\Delta_{\rm EDM}$ is completely governed by the EDM stress history, which we quantify using the two variables Δ_p and Δ_π. These same two variables also control the evolution of gravitational potential, which is important for the CMB power spectrum. This implies that the CMB is an ideal test bed for EDM models. In reality, we have one more freedom because once the $\Delta_{\rm EDM}(a)$ is specified. Equation (35) becomes a single equation for the two variables Δ_p and Δ_π, so, in Sec. IV, we considered three separate cases: (I) $\Delta_\pi = 0$, $\Delta_p \neq 0$, (II) $\Delta_\pi \neq 0$, $\Delta_p = 0$, and (III) $\Delta_\pi \neq 0$, $\Delta_p \neq 0$. For simplicity, we have also made the following assump-

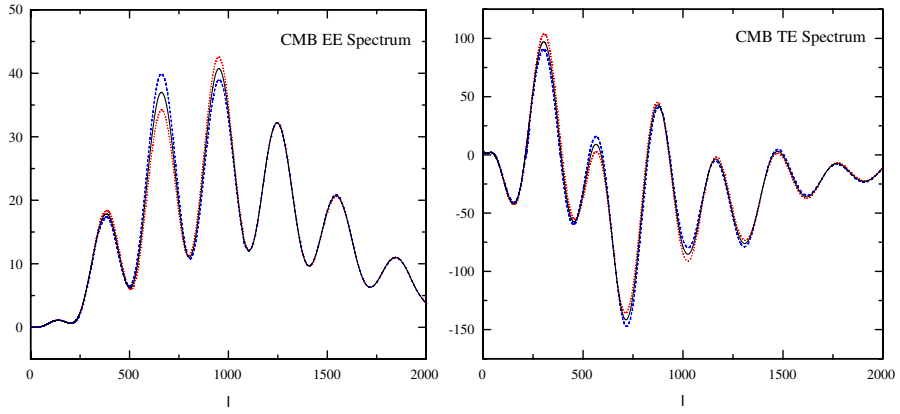

FIG. 8 (color online). (color online) The CMB polarization spectra for the model with the same parameters as in Fig. 7. The red dotted, black solid, and blue dashed curves are the cases $b = 0.8$, 1.0, 1.2, respectively.

tions: (1) the evolution of $\Delta_{\rm EDM}$ is scale independent, as is implied by the observed LSS, (2) the cosmological constant (or other form of explicit dark energy violating the strong energy condition) is neglected to simplify the numerics, (3) the EDM equation of state parameter, $w_{\rm EDM}$, is assumed to be small enough so that we can assume the standard CDM background evolution holds; and, (4) only adiabatic initial conditions, a scale-independent $n_s = 1$ primordial power spectrum, and effectively massless neutrinos are considered (we will return to these assumptions below).

For case I, the standard CDM relation $\Psi = -\Phi = \phi$ still holds, but the evolution of these potentials could be changed. If the deviation of EDM from CDM only occurs after the last scattering, then this change in ϕ mainly modifies the ISW effect and, hence, the low-ℓ CMB power. If the EDM starts to deviate from CDM before last scattering, however, then the early changes in Ψ and Φ would modify the CMB acoustic peak features in a complicated manner, as we described qualitatively in Secs. III and IV A. The evolution of Δ_p can be understood qualitatively: since the effect of the pressure perturbation is to counteract gravitational collapse, in order that $\Delta_{\rm EDM}$ grows faster than $\Delta_{\rm CDM}$ we need a negative Δ_p, and vice versa (c.f. Fig. 6).

The case II evolution is problematic as long as we stick to the above simplifying assumption (1), i.e., requiring a scale-independent growth of $\Delta_{\rm EDM}$, because in this case Eq. (35) implies a scale *dependent* Δ_π ($k^2\Delta_\pi$ is independent of k), which diverges on large scales (small k). As we have seen in Sec. IV B, this leads to a strong late-ISW effect, blowing up the low-ℓ CMB spectrum even if the EDM only differs slightly from standard CDM. Furthermore, a natural EDM model with $\Delta_p = 0$ and $\Delta_\pi \neq 0$ does not exist in the literature, and this model is different from case I, which arises naturally in $f(K)$ models with $c_{13} = 0$.

Of course, the most general situation is our case III, where both Δ_p and Δ_π are nonzero. Needless to say, this generality also makes its exploration more difficult. One could, however, use the extra degree of freedom here in model constructions. If we fix *both* the evolution of $\Delta_{\rm EDM}(a)$ *and* that of the potential ϕ, then Δ_π and Δ_p can be solved uniquely at the same time. Such a construction has the advantage that we can fix the evolution of ϕ to be identical to that in standard CDM so that the ISW effect is not changed at all. If the deviation of EDM starts after last scattering, then such a model is degenerate with standard CDM even after CMB and LSS data are taken into account, and furthermore the CMB-galaxy cross-correlation data is inefficient in constraining it. Allowing EDM to deviate before last scattering, however, will almost surely predict different CMB peak features, because in this case $\Psi \neq -\Phi \neq \phi$ and the acoustic oscillations of photon-baryon fluid are changed with respect to standard CDM (c.f. Sec. III). Dropping the requirement on the evolution of ϕ makes the situation even worse, because in this case the ISW effect and low-ℓ structure of the CMB spectrum are also changed. We stress that the CMB polarization also provides invaluable information for constraining EDM models, because it depends only on the quadrupole moment of the photon temperature perturbation Θ (the photon anisotropic stress), and thus only on the physics close to the time of last scattering.

Throughout this paper we have chosen to parametrize $\Delta_{\rm EDM}(a)$ as in Eq. (43). This is fairly simple and sufficient for our purposes as we only aim to show the importance of CMB data in constraining alternative gravitational dark-matter theories, but not to constrain any specified model or given parametrization exactly. There are good reasons why more detailed parametrizations are needed for more precise future studies. First, although $\Delta_{\rm CDM} \propto a$ is a good approximation in the matter-dominated epoch, it breaks down when the contribution from radiation is still significant (including the time prior to and around last scattering) and when a cosmological constant is included. Second, because the physics at the time of matter-radiation equality is relevant for EDM models, which deviate from CDM earlier, we sometimes need to choose a_i to be smaller than the matter-radiation equality $a_{\rm eq}$, which means that the evolution of $\Delta_{\rm EDM}(a)$ or $\Delta_{\rm CDM}(a)$ cannot be completely scale independent (remember that $a_{\rm eq}$ is relevant for the bending of the matter power spectrum [76]). Thus, future precise calculations, particularly those relevant for weak lensing and the galaxy-ISW cross correlation, should use parametrizations that reduce exactly to $\Delta_{\rm CDM}(a)$ in the ΛCDM model in appropriate limits.

Notice that our logic here is different from other related considerations of generalized dark matter (GDM) [60,77]. In Ref. [77], for example, the author parametrizes the stress sector of the GDM with three quantities, w_g, $c^2_{\rm eff}$, and $c^2_{\rm vis}$, which, respectively, characterize the equation of state, pressure perturbation, and anisotropic stress of the GDM. The GDM effects on the CMB *and* matter power spectra are then studied by assuming some specific values of these quantities. Our approach tackles the problem from a different direction and is therefore complementary to those earlier works.

One interesting issue is the inclusion of hot dark matter, which is needed by TeVeS itself. This can certainly be achieved by setting special values for w_g, $c^2_{\rm eff}$, and $c^2_{\rm vis}$ as in [77]. In our approach, we simply treat the EDM as a "black box," which is completely controlled by separate conservation equations. By parametrizing $\Delta_{\rm EDM}(a)$, we are able to extract information on the pressure perturbation Δ_p and anisotropic stress Δ_π from these conservation equations without knowing exactly what is in the box—it can be mixtures of modified gravitational effects and neutrinos, or something else entirely.

The other issue is related to the initial conditions. In this work we mainly focus on the adiabatic initial conditions as

in [77]. However, it is well known that the adiabatic initial condition is far from the only possibility, and there can be four regular isocurvature modes [78]. These isocurvature modes are predicted by many theoretical models and may even correlate with the adiabatic one. In contrast to the adiabatic mode, the isocurvature mode excites sinusoidal oscillations of the photon-baryon fluid and so predicts the first CMB acoustic peak to be around $\ell \sim 330$ rather than 220; consequently, a pure or dominating isocurvature initial condition is incompatible with basic CMB observations. Nonetheless, a subdominant contribution from isocurvature initial conditions actually degenerates with other cosmological parameters and cannot be ruled out by the current data [79–82]. In our EDM model, if the EDM evolves differently from CDM early in the radiation era, then $\Delta_{\rm EDM}$ does not evolve adiabatically, and the entropy perturbation $S_{\rm EDM} = \Delta_{\rm EDM} - \frac{3}{4}\Delta_\gamma$ is nonzero. In this case, one might naturally expect that there should be isocurvature modes in the initial conditions. A detailed calculation of the consequences of introducing such modes, however, generally requires thorough searches of the new parameter space (which is enlarged compared with the standard case, because now the amplitude, tilt of the isocurvature modes and their correlation with the adiabatic mode must be taken as free parameters) like in [79–82] and is beyond the scope of this work. Moreover, allowing different initial conditions (especially tilts of the isocurvature mode, which are significantly different from 1) can change the shape of matter power spectrum, which means that the parametrization of $\Delta_{\rm EDM}(a)$ [c.f. Eq. (43)] should be scale dependent for the same reasons as discussed above. In this work, we adopt a more conservative approach by assuming that the EDM evolves like standard CDM at earlier times and so adiabaticity is a natural choice.

In conclusion, we propose ways to use the CMB in order to constrain those alternative gravity theories for dark matter, which claim to be compatible with the observed LSS. We find that the CMB temperature and polarization spectra are good discriminators between these theories in general, especially when they deviate from the CDM paradigm before last scattering. If the deviation starts after last scattering, however, there can exist EDM theories that are degenerate with respect to the standard ΛCDM model and cannot be distinguished by CMB and matter power spectra. This point is particularly interesting from the viewpoint of model constructions. Our results also indicate that the stress properties of dark matter, which determine the evolutions of both density perturbations and gravitational potential, can be studied and significantly constrained with existing and future data by using just the general conservation equations and without specializing to any specific theoretical model.

ACKNOWLEDGMENTS

We thank David Spergel for helpful discussions. The numerical calculation of this work uses a modified version of the CAMB code [83]. B. L. thanks the University of St. Andrews for its hospitality where part of this work was carried out and acknowledges supports from an Overseas Research Studentship, the Cambridge Overseas Trust, the DAMTP, and Queens' College at Cambridge. D. F. M. acknowledges the Humboldt Foundation.

[1] S. M. Carroll, A. De Felice, V. Duvvuri, D. A. Easson, M. Trodden, and M. S. Turner, Phys. Rev. D **71**, 063513 (2005).
[2] D. A. Easson, Int. J. Mod. Phys. A **19**, 5343 (2004).
[3] D. N. Vollick, Phys. Rev. D **68**, 063510 (2003).
[4] A. W. Brookfield *et al.*, Phys. Rev. D **73**, 083515 (2006).
[5] G. Allemandi, A. Borowiec, and M. Francaviglia, Phys. Rev. D **70**, 043524 (2004).
[6] G. Allemandi, A. Borowiec, and M. Francaviglia, Phys. Rev. D **70**, 103503 (2004).
[7] S. Nojiri and S. D. Odintsov, Phys. Lett. B **631**, 1 (2005).
[8] M. Amarzguioui *et al.*, Astron. Astrophys. **454**, 707 (2006).
[9] S. Nojiri, S. D. Odintsov, and O. G. Gorbunova, J. Phys. A **39**, 6627 (2006).
[10] J.-P. Uzan, Phys. Rev. D **59**, 123510 (1999).
[11] T. Chiba, Phys. Lett. B **575**, 1 (2003).
[12] A. L. Erickcek, T. L. Smith, and M. Kamionkowski, Phys. Rev. D **74**, 121501 (2006).
[13] I. Navarro and K. V. Acoleyen, J. Cosmol. Astropart. Phys. 02 (2007) 022.
[14] T. Faulkner, M. Tegmark, E. F. Bunn, and Y. Mao, Phys. Rev. D **76**, 063505 (2007).
[15] E. Barausse, T. P. Sotiriou, and J. C. Miller, Classical Quantum Gravity **25**, 062001 (2008).
[16] W. Hu and I. Sawicki, Phys. Rev. D **76**, 064004 (2007).
[17] G. J. Olmo, Phys. Rev. Lett. **95**, 261102 (2005).
[18] T. Koivisto, Phys. Rev. D **73**, 083517 (2006).
[19] B. Li and M.-C. Chu, Phys. Rev. D **74**, 104010 (2006).
[20] B. Li, K.-C. Chan, and M.-C. Chu, Phys. Rev. D **76**, 024002 (2007).
[21] B. Li and J. D. Barrow, Phys. Rev. D **75**, 084010 (2007).
[22] B. Li, J. D. Barrow, and D. F. Mota, Phys. Rev. D **76**, 044027 (2007).
[23] B. Li, J. D. Barrow, and D. F. Mota, Phys. Rev. D **76**, 104047 (2007).
[24] L. Amendola, D. Polarski, and S. Tsujikawa, Phys. Rev. Lett. **98**, 131302 (2007).
[25] B. Li, D. F. Mota, and D. J. Shaw, arXiv:0801.0603.
[26] B. Li, D. F. Mota, and D. J. Shaw, arXiv:0805.3428.

[27] W. Hu and I. Sawicki, Phys. Rev. D **76**, 064004 (2007).
[28] D. F. Mota and D. J. Shaw, Phys. Rev. D **75**, 063501 (2007).
[29] D. F. Mota and D. J. Shaw, Phys. Rev. Lett. **97**, 151102 (2006).
[30] J. Khoury and A. Weltman, Phys. Rev. D **69**, 044026 (2004).
[31] S. A. Appleby and R. A. Battye, Phys. Lett. B **654**, 7 (2007).
[32] L. Amendola and S. Tsujikawa, Phys. Lett. B **660**, 125 (2008).
[33] B. Jain and P. Zhang, arXiv:0709.2375.
[34] D. F. Mota, J. R. Kristiansen, T. Koivisto, and N. E. Groeneboom, Mon. Not. R. Astron. Soc. **382**, 793 (2007).
[35] W. Hu and I. Sawicki, Phys. Rev. D **76**, 104043 (2007).
[36] E. Bertschinger and P. Zukin, Phys. Rev. D **78**, 024015 (2008).
[37] W. Hu, Phys. Rev. D **77**, 103524 (2008).
[38] J.-P. Uzan and F. Bernardeau, Phys. Rev. D **64** 083004 (2001);See also J.-P. Uzan arXiv: astro-ph/0605313; C. Schimd, J.-P. Uzan, and A. Riazuelo, Phys. Rev. D **71**, 083512 (2005).
[39] M. Milgrom, Astrophys. J. **270**, 365 (1983); **270**, 371 (1983); **270**, 384 (1983).
[40] J. D. Bekenstein, Phys. Rev. D **70**, 083509 (2004).
[41] C. Skordis *et al.*, Phys. Rev. Lett. **96**, 011301 (2006); C. Skordis, Phys. Rev. D **74**, 103513 (2006).
[42] S. Dodelson and M. Liguori, Phys. Rev. Lett. **97**, 231301 (2006).
[43] H. Zhao, D. J. Bacon, A. N. Taylor, and K. Horne, Mon. Not. R. Astron. Soc. **368**, 171 (2006).
[44] H. Shan, M. Feix, B. Famaey, and H. Zhao, arXiv:0804.2668 [Mon. Not. R. Astron. Soc. (to be published)].
[45] O. Tiret and F. Combes, Astron. Astrophys. **464**, 517 (2007).
[46] G. Gentile, H. Zhao, and B. Famaey, arXiv:0712.1816.
[47] O. Gnedin and H. Zhao, Mon. Not. R. Astron. Soc. **333**, 299 (2002).
[48] T. Jacobson and D. Mattingly, Phys. Rev. D **64**, 024028 (2001); C. Eling, T. Jacobson, and D. Mattingly, arXiv:gr-qc/0410001.
[49] T. G. Zlosnik, P. G. Ferreira, and G. D. Starkman, Phys. Rev. D **74**, 044037 (2006).
[50] P. G. Ferreira, B. M. Gripaios, R. Saffari, and T. G. Zlosnik, Phys. Rev. D **75**, 044014 (2007).
[51] T. G. Zlosnik, P. G. Ferreira, and G. D. Starkman, Phys. Rev. D **75**, 044017 (2007).
[52] B. Li, D. F. Mota, and J. D. Barrow, Phys. Rev. D **77**, 024032 (2008).
[53] T. Koivisto and D. F. Mota, J. Cosmol. Astropart. Phys. 06 (2008) 018.
[54] F. Bourliot, P. G. Ferreira, D. F. Mota, and C. Skordis, Phys. Rev. D **75**, 063508 (2007).
[55] H. Zhao, arXiv:0710.3616 [Astrophys. J. Lett. (to be published)].
[56] C. Skordis, Phys. Rev. D **77**, 123502 (2008).
[57] A. Halle, H. Zhao, and B. Li, [Astrophys. J. Suppl. Ser. (to be published)]; H. Zhao and B. Li, arXiv:0804.1588.
[58] T. G. Zlosnik, P. G. Ferreira, and G. D. Starkman, Phys. Rev. D **77**, 084010 (2008).
[59] G. R. Ellis and M. Bruni, Phys. Rev. D **40**, 1804 (1989); G. F. R. Ellis and H. Van Elst, in *Theoretical and Observational Cosmology*, edited by M. Lachièze-Rey (Springer, New York, 1998); A. Challinor and A. Lasenby, Astrophys. J. **513**, 1 (1999); A. M. Lewis, Ph.D. dissertation, Queens' College and Astrophysics Group, Cavendish Laboratory, Cambridge University, 2000.
[60] W. Hu and D. J. Eisenstein, Phys. Rev. D **59**, 083509 (1999).
[61] W. Hu, N. Sugiyama, and J. Silk, Nature (London) **386**, 37 (1997).
[62] W. Hu and S. Dodelson, Annu. Rev. Astron. Astrophys. **40**, 171 (2002).
[63] W. Hu, arXiv:0802.3688.
[64] S. Dodelson, *Modern Cosmology* (Academic Press, London, 2003).
[65] W. Hu and N. Sugiyama, Astrophys. J. **444**, 489 (1995).
[66] D. N. Spergel *et al.*, Astrophys. J. Suppl. Ser. **170**, 377 (2007).
[67] C. L. Reichardt *et al.*, arXiv:0801.1491.
[68] R. Caldwell, A. Cooray, and A. Melchiorri, Phys. Rev. D **76**, 023507 (2007).
[69] W. Hu and R. Scranton, Phys. Rev. D **70**, 123002 (2004).
[70] F. Schmidt, M. Liguori, and S. Dodelson, Phys. Rev. D **76**, 083518 (2007).
[71] B. M. Schafer, G. A. Caldera-Cabral, and R. Maartens, arXiv:0803.2154.
[72] W. Hu and M. White, Phys. Rev. D **56**, 596 (1997).
[73] W. Hu and M. White, New Astron. Rev. **2**, 323 (1997).
[74] J. Kovac *et al.*, Nature (London) **420**, 772 (2002).
[75] C. Bischoff *et al.*, arXiv:0802.0888.
[76] A. R. Liddle, A. Mazumdar, and J. D. Barrow, Phys. Rev. D **58**, 027302 (1998).
[77] W. Hu, Astrophys. J. **506**, 485 (1998).
[78] M. Bucher, K. Moodley, and N. Turok, Phys. Rev. D **62**, 083508 (2000).
[79] R. Trotta, A. Riazuelo, and R. Durrer, Phys. Rev. Lett. **87**, 231301 (2001).
[80] L. Amendola, C. Gordon, D. Wands, and M. Sasaki, Phys. Rev. Lett. **88**, 211302 (2002).
[81] M. Beltrán, J. García-Bellido, J. Lesgourgues, and A. Riazuelo, Phys. Rev. D **70**, 103530 (2004).
[82] R. Keskitalo, H. Kurki-Suonio, V. Muhonen, and J. Väliviita, J. Cosmol. Astropart. Phys. 09 (2007) 008.
[83] A. M. Lewis, A. Challinor, and A. Lasnenby, Astrophys. J. **538**, 473 (2000), See also http://camb.info/.